High-pressure X-ray diffraction studies of organic anhydrides

Tomasz Poręba

European Synchrotron Radiation Facility, 71 Av. des Martyrs, 38000 Grenoble, France

Introduction

Maleic anhydride (MA) and its derivatives are compounds of great commercial importance. Next to acetic and phthalic anhydride, maleic anhydride is the second most important anhydride in commercial use.[1] They find applications in nearly every field of industrial chemistry. They are classic substrates for Diels-Alder reactions and are used, for example, as curing agents in epoxy resins.[2] In addition, these anhydrides are important raw materials used in the production of phthalic-type alkyd and unsaturated polyester resins (UPR), surface coatings, lubricant additives, copolymers, and agricultural chemicals.[3] Often Diels-Alder reactions and polymerization of maleic anhydride or its derivatives are carried out using high pressure methods,[4–6] that have become increasingly attractive, also in synthetic organic chemistry.[7,8] High-pressure studies often lead to the observation of interesting effects, it can reduce the sample volume and compress the intermolecular contacts to values unattainable by other methods or even initiate chemical reactions. The compressed materials reveal new information about intermolecular interactions and new phases can be obtained.[9,10] Therefore, it is extremely important to know the effect of high-pressure on the structure and properties of maleic anhydride and its derivatives, which was the main purpose of my project. Using synchrotron X-ray diffraction, I investigated the structure and properties of the α- and β-phases of 2,3-diphenyl maleic anhydride (DPMA) (Fig. 1a) under high pressure. To generate high-pressure we have used diamond anvil cell. We described the structure of *α*-DPMA up to 12.29 GPa and *β*-DPMA up to 10.73 GPa.

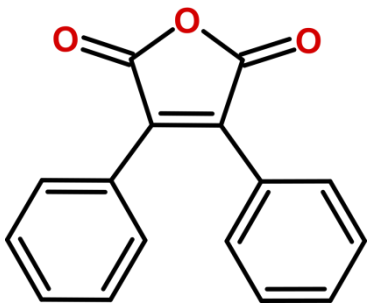

Figure 1. Structural formula of 2,3-diphenyl maleic acid anhydride (DPMA).

DPMA crystals were first described by Jenssen in 1893.[11] and then the polymorphism, crystal morphology and fluorescence of this compound were reported by Drugman in 1912.[12] He determined the melting points of the polymorphs, described that the α-phase is orthorhombic, the β-phase is monoclinic, and also he derived the lattice parameter ratios (Table 1). He did it a year before the first crystal stucture was determined using X-ray diffraction by Bragg,[13] which is why DPMA is called a „historical'' compound.[14] The structure of α-DPMA was then determined at atmospheric pressure using X-ray diffraction techniques in 1995 by Yoon *et al*.[15] In 2005, the structure was redetermined and compared to the β-DPMA structure by Klapper *et al*.[14] At ambient conditions, stable, orthorombic α-phase of DPMA (m.p. = 156 °C, ρ = 1.334 g/cm^3) crystallizes in space group *P*bca, whereas the metastable, monoclinic β-phase (m.p. = 146 °C, ρ = 1.350 g/cm^3) in the space group $P2_1/c$. Subsequently, DPMA luminescence studies were also performered by Ling *et al.*[16]

Table 1. Properties of α- and β-polymorphs described by Drugman.[12,14]

Parameter	α-DPMA	β-DPMA
Crystal system	orthorhombic	monoclinic
Axis ratio a : b : c	0.5176 : 1 : 0.7024	2.561 : 1 : 2.327
Monoclinic angle	-	101°33'
Density [g/cm^3]	1.340	1.345
Melting point [°C]	155	146

Experimental

High-pressure experiments were performed using a membrane-type diamond-anvil cell (DAC) (Fig. 1).[17] This simple and small device is build of two diamonds in the parallel position, separated by the metal gasket, where the sample is placed. There are many advantages to using diamonds to exert pressure. DAC chamber allows to generate pressure several thousand times higher than on Earth's Surface, it is possible to observe the sample during experiments, perform structural studies using X-ray diffraction or spectroscopic studies such as Raman or UV-Vis.

To conduct the experiment, the DAC chamber was prepared as follows:

(i) using a laser, a hole was drilled in the steel gasket;

(ii) the gasket was cleaned, placed between two diamond culets, centered, and pre-indented to 70 μm;

(iii) two single DPMA crystals, α and β phase, a ruby sphere (used for pressure calibration), and a small piece of gold (used to center the DAC chamber during X-ray diffraction measurements) were placed inside the gasket;

(iv) the DAC chamber was filled with helium as a pressure transmitting medium.

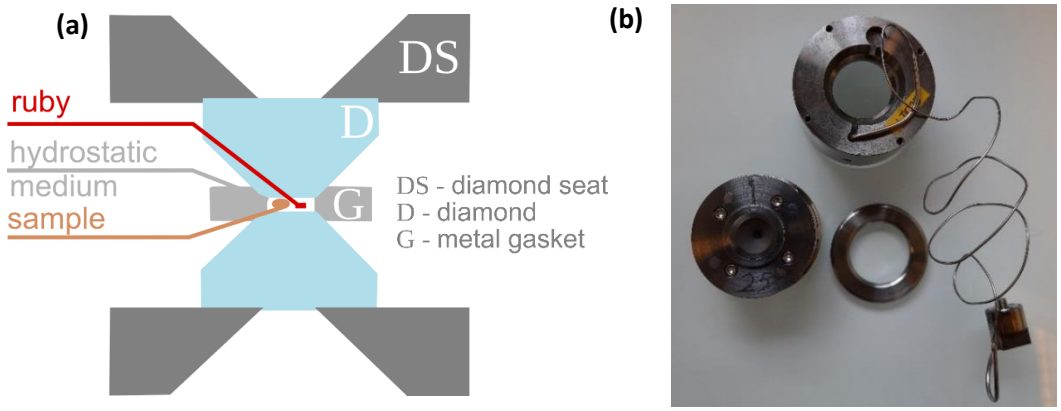

Figure 2. (a) A schematics cross section of the DAC; and (b) a mambrane type diamond anvil cell.

Pressure was calibrated using a ruby fluorescence method.[18,19] The ruby sphere was placed inside a gasket, irradiated with a laser (λ = 532 nm), and then the detector measured its fluorescence (Fig. 2a). An excitation signal R1 at ambient conditions occurs at about 694.34 nm, due to a presence of Cr^{3+} ions, and is linearly shifted as a function of pressure (Fig. 2b). In constant temperature of the measurement pressure, inside the DAC chamber, can be

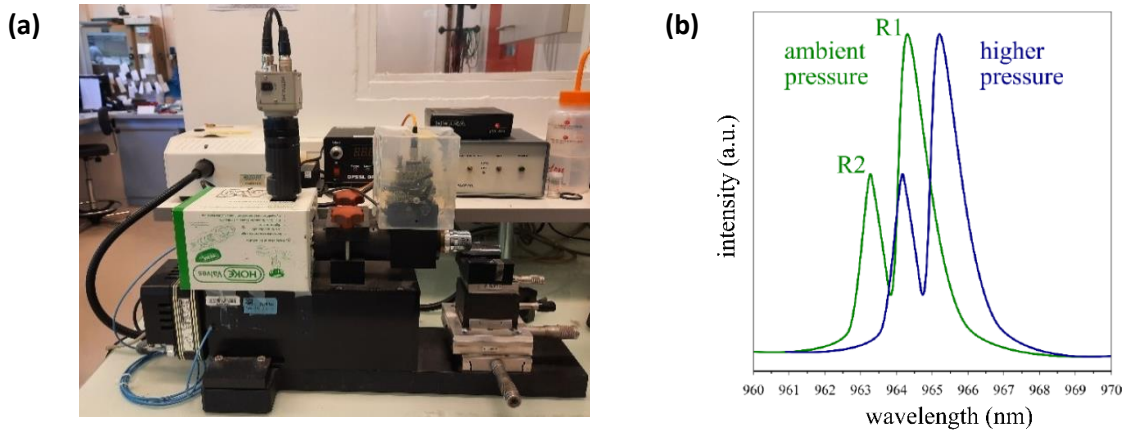

determined with an accuracy of 0.02 GPa.

Figure 3. Spectrometer used to measure and calibrate pressure; (b) ruby fluorescence spectrum, with R1 and R2 lines that linearly shift toward higher wavelengths at high pressure.

The structures of high-pressure phases were determined by in-situ single-crystal synchrotron X-ray diffraction. The experiments were performed at beamline ID15B at the European Synchrotron Radiation Facility (ESRF) in Grenoble (Fig. 3a). After the pressure was increased in the range of 0.2-0.85 GPa each time, X-ray diffraction measurements of two crystals (α- and β-DPMA) were then performed (Rys. 3b). The CrysAlisPro software[20] was used for collecting diffraction data and their reduction. The crystal structures were solved by the direct methods with program SHELXS and refined by least-squares with SHELXLby using Olex2 software.[21–23] Structural drawings were prepared using Mercury program.[24]

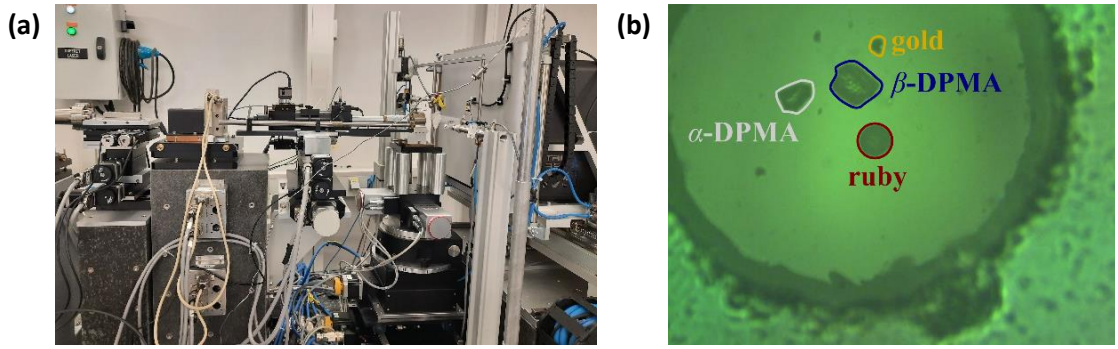

Figure 4. (a) Beamline ID15b with a diamond anvil cell mounted and prepared for measurement; (b) DAC chamber at 0.394 GPa.

Results and discussion

As a result of X-ray diffraction measurements, we determined the structure of α-DPMA up to 12.29 GPa and β-DPMA up to 10.73 GPa. Selected crystallographic data are shown in Table 2 and Table 3, respectively. The compressibility plots of α- and β-DPMA are shown in Figure 5.

Table 2. Selected crystallographic data of α-DPMA with increasing pressure.

pressure (GPa)	*a* (Å)	*b* (Å)	*c* (Å)	*V* (Å^3)	*Z*/*Z*'
0.394	18.8413(19)	13.016(3)	19.5156(19)	4786.1(13)	16/2
0.676	18.7082(13)	12.748(2)	19.3964(13)	4625.8(9)	16/2
1.013	18.6090(14)	12.532(2)	19.3103(13)	4503.2(9)	16/2
1.303	18.5396(12)	12.383(2)	19.2418(12)	4417.4(8)	16/2
1.587	18.4805(13)	12.256(2)	19.1882(12)	4346.1(8)	16/2
1.952	18.4169(10)	12.1227(16)	19.1295(9)	4270.9(6)	16/2
2.31	18.3470(10)	12.0029(17)	19.0756(10)	4200.8(7)	16/2
2.95	18.2778(11)	11.8657(17)	19.0166(10)	4124.3(7)	16/2
3.142	18.2406(9)	11.7915(14)	18.9819(8)	4082.7(6)	16/2
3.659	18.1815(9)	11.6848(15)	18.9273(9)	4021.1(6)	16/2
4.38	18.0953(9)	11.5249(14)	18.8492(8)	3930.9(5)	16/2
5.24	18.0189(10)	11.3833(17)	18.7789(8)	3851.8(6)	16/2

5.75	17.9722(12)	11.2989(14)	18.7274(9)	3802.9(6)	16/2
6.39	17.9207(9)	11.2118(14)	18.6787(8)	3753.0(5)	16/2
7.22	17.8624(9)	11.1108(14)	18.6195(9)	3695.3(5)	16/2
8.01	17.8005(8)	11.0119(13)	18.5584(8)	3637.8(5)	16/2
8.75	17.7483(7)	10.9243(11)	18.5124(7)	3589.3(4)	16/2
9.32	17.7138(8)	10.8699(11)	18.4801(7)	3558.3(4)	16/2
9.95	17.6800(8)	10.8161(10)	18.4417(6)	3526.6(4)	16/2
10.73	17.6398(7)	10.7553(10)	18.3977(7)	3490.4(4)	16/2
11.45	17.5910(7)	10.6903(11)	18.3509(7)	3450.9(4)	16/2
12.29	17.5388(7)	10.6084(10)	18.2975(7)	3404.4(4)	16/2

Table 3. Selected crystallographic data of β-DPMA with increasing pressure.

pressure (GPa)	***a* (Å)**	***b* (Å)**	***c* (Å)**	***β* (°)**	***V* (Å^3)**	**Z/Z'**
0.394	15.042(9)	5.8818(4)	13.7004(11)	101.96(2)	1185.8(7)	4/1
0.676	14.916(6)	5.8175(3)	13.5664(8)	102.405(17)	1149.7(5)	4/1
1.013	14.810(6)	5.7628(3)	13.4467(8)	102.772(16)	1119.3(5)	4/1
1.303	14.724(6)	5.7299(3)	13.3800(8)	102.982(18)	1100.0(5)	4/1
1.587	14.661(5)	5.6974(2)	13.3088(8)	103.181(16)	1082.4(4)	4/1
1.952	14.587(5)	5.6643(2)	13.2382(8)	103.385(16)	1064.1(4)	4/1
2.31	14.521(5)	5.6322(2)	13.1708(8)	103.552(14)	1047.2(3)	4/1
2.95	14.429(5)	5.5996(2)	13.0993(7)	103.725(15)	1028.2(3)	4/1
3.142	14.120(5)	5.5974(3)	12.8042(6)	92.088(12)	1011.3(4)	4/1
3.659	14.020(5)	5.5844(3)	12.7370(8)	92.283(13)	996.4(3)	4/1
4.38	17.562(3)	5.7546(2)	47.943(6)	91.025(14)	4844.3(9)	20/5
5.24	17.3110(15)	5.74710(10)	47.729(4)	91.377(9)	4747.1(6)	20/5
5.75	17.1698(15)	5.74040(10)	47.593(4)	91.530(9)	4689.2(6)	20/5
6.39	17.0129(15)	5.73290(10)	47.452(3)	91.719(8)	4626.1(5)	20/5
7.22	16.7367(18)	5.75420(10)	47.350(4)	93.600(10)	4551.1(6)	20/5
8.01	16.5598(14)	5.74610(10)	47.185(3)	93.865(8)	4479.7(5)	20/5
8.75	16.4195(14)	5.73560(10)	47.060(3)	94.142(8)	4420.4(5)	20/5
9.32	16.3257(14)	5.72990(10)	46.969(3)	94.256(8)	4381.6(5)	20/5
9.95	16.2293(14)	5.72360(10)	46.885(3)	94.397(9)	4342.3(5)	20/5
10.73	16.1208(12)	5.71490(10)	46.772(3)	94.570(7)	4295.4(4)	20/5

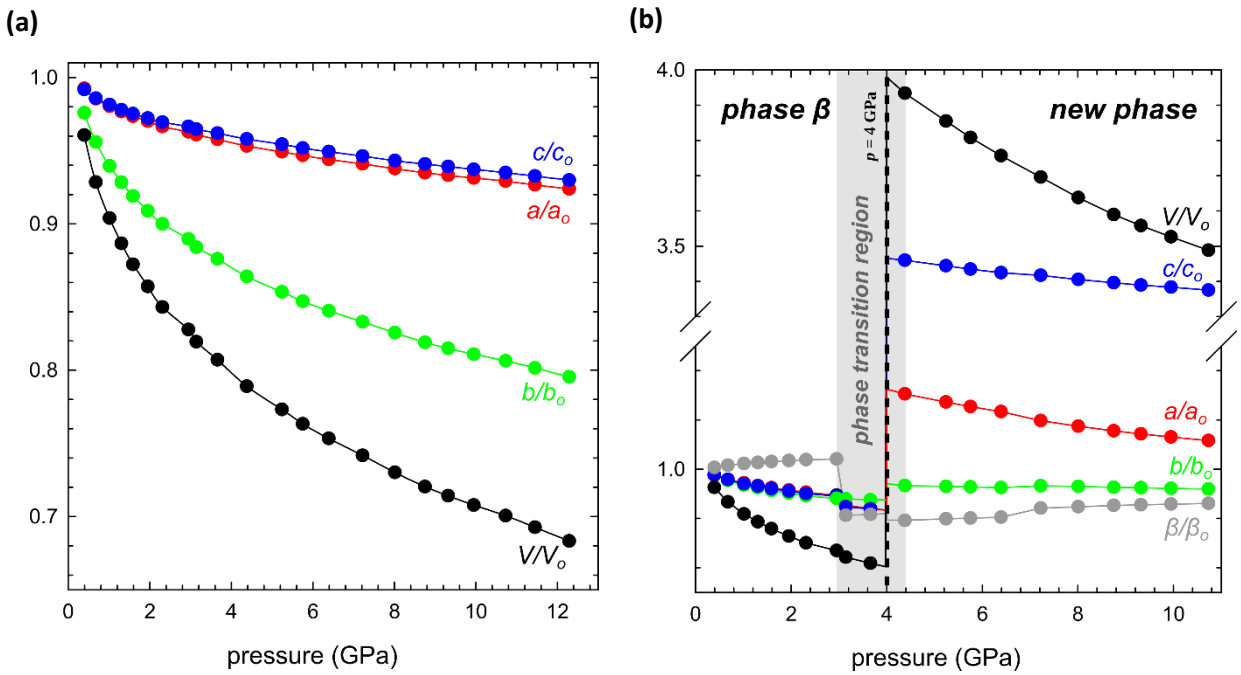

Figure 5. Compression of the unit-cell parameters with increasing pressure for phases (a) α; and (b) β of DPMA, in relation to the average unit-cell dimensions (a_o, b_o, c_o, V_o) at atmospheric pressure. The estimated standard deviations (ESDs) are smaller than the symbols.

α-DPMA

The α-polymorph, the same as at atmospheric pressure, crystallizes in the space group *P*bca with two symmetry independent molecules (Z' = 2). There are eight A and eight B molecules in the unit cell. The layers of molecules A and B are arranged alternately, parallel to the (010) lattice plane (Fig. 6). For α-DPMA, up to 12.29 GPa, we did not observe a phase transition. A plot showing the compressibility of the unit-cell parameters is shown in Figure 4a. The α-DPMA crystal is most compressed along [y], while the compression of the crystal along [x] and [z] are similar. This can also be seen in the projections of the unit-cell in three directions (Fig. 7); there are free spaces along the b-axis that allow the greatest compression in that direction.

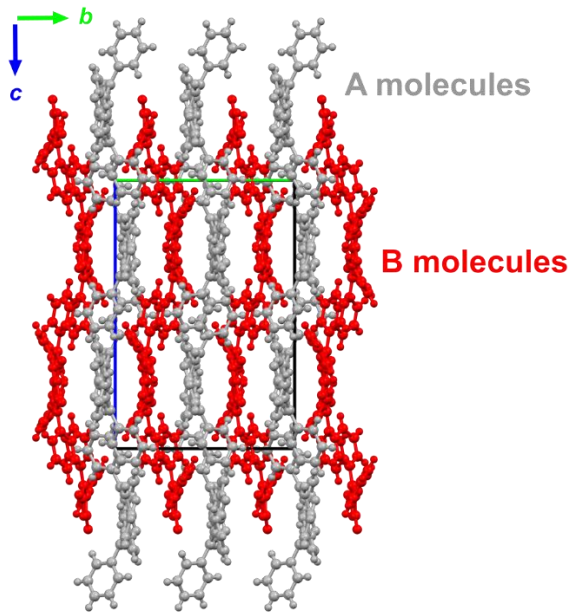

Figure 6. Arrangement of alternating layers of molecules A and B in the α-DPMA crystal in the direction [100].

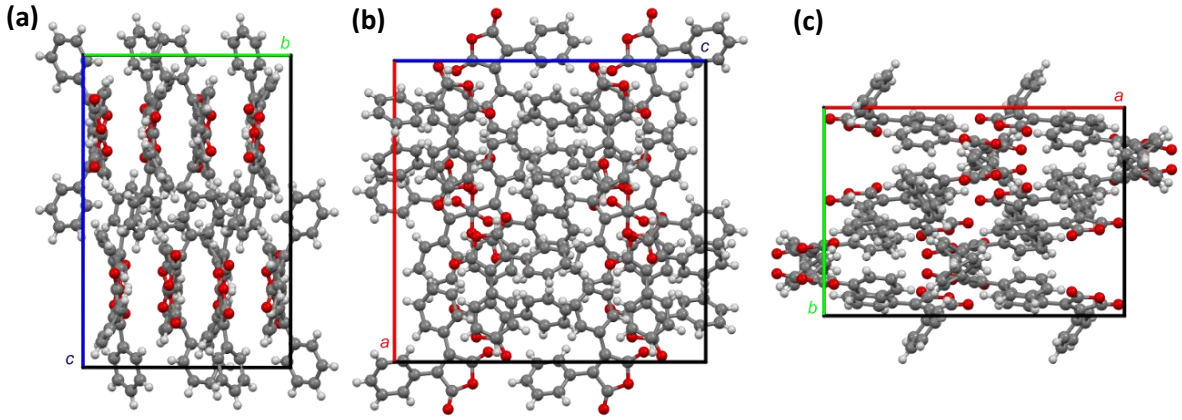

Figure 7. Arrangements of α-DPMA molecules in the unit-cell along direction: (a) [100]; (b) [010]; and (c) [001], at 0.394 GPa.

β-DPMA

β-DPMA crystallizes in the monoclinic space group $P2_1/c$. In the structure under ambient conditions, there is one symmetry-independent molecule in the unit-cell (Z' = 1). At 4 GPa, there is a phase transition. Interestingly, a few measurements earlier, before the phase transition, at approximately 3 GPa we observed a sudden decrease in the β-angle, while the other parameters do not change significantly. This point starts the phase transition region (Fig. 5b). The transition results in a more than 3-fold extension of the c-edge, and the number of independent molecules in the unit cell (Z') increases from 1 to 5 (Fig. 8). The space group remains the same, that is $P2_1/c$.

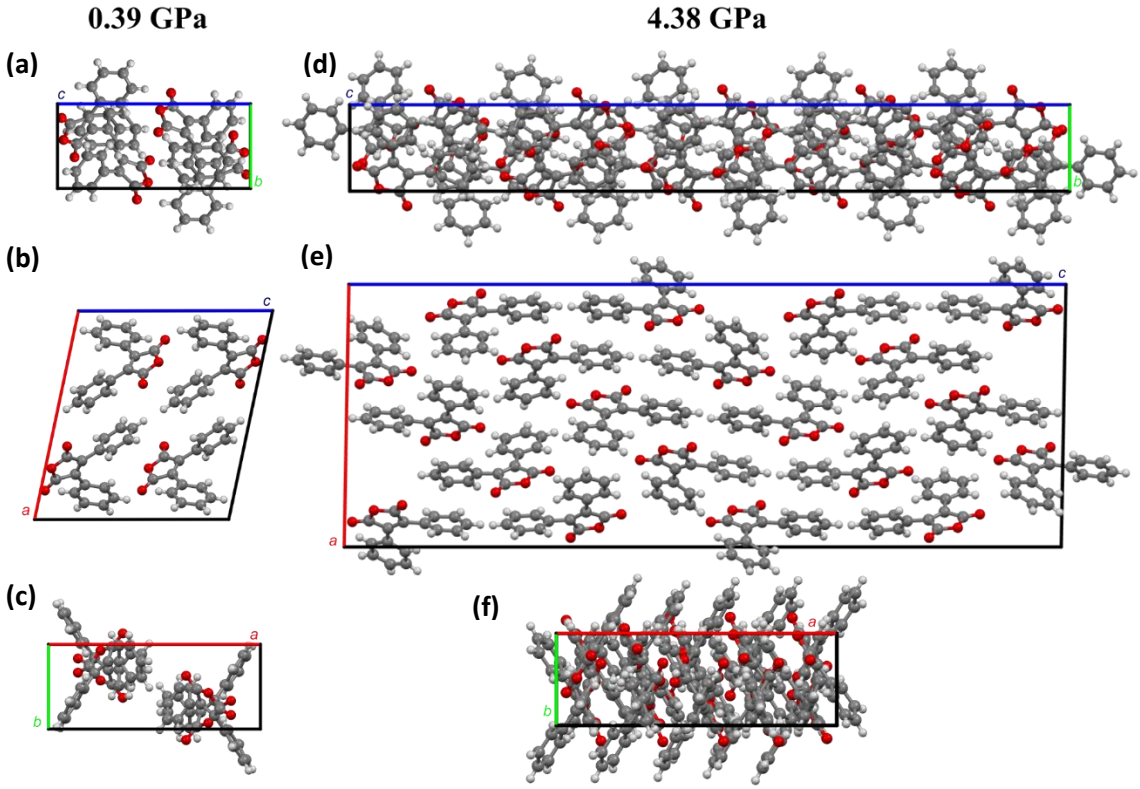

Figure 8. Arrangements of DPMA molecules in the unit-cell in three directions; *β*-DPMA at 0.394 GPa along direction: (a) [100]; (b) [001]; and (c) [001]; and new phase at 4.38 GPa: (d) [100]; (e) [010]; and (f) [001].

Fluorescence

DPMA crystals exhibit fluorescent properties (Fig. 9a and 9b) and it is due to the conjugated B-system of molecule.[14] DPMA exhibits aggregation-induced emission (AIE), meaning that it shows very weak fluorescence in low-viscosity organic solvents and exhibits intense fluorescence in high-viscosity or in its aggregation/solid-state.[16,25] At ambient conditions, under UV radiation the two polymorphs of DPMA show a strong blue luminescence (Fig. 9b). Also during the pressure measurements inside the DAC chamber, we could observe strong fluorescence of the *β*-DPMA crystal. The color of the crystal changed from yellow to black as the pressure increased (Fig. 9a). This means that the change in molecular packing with increasing pressure significantly affects the fluorescence of this compound. According to Molecular Orbital Theory, the observed bathochromic shift increasing pressure is due to a reduction in the gap between the Highest Occupied Molecular Orbital (HOMO) and the Lowest Unoccupied Molecular Orbital (LUMO) (Fig. 9c).

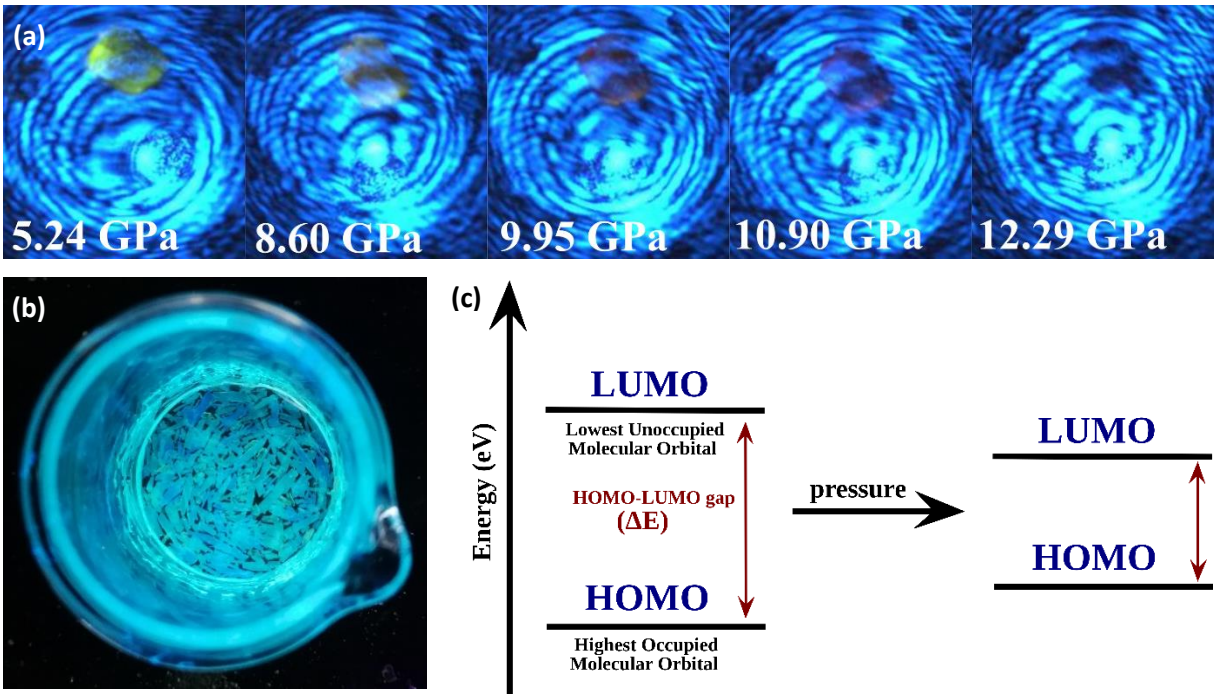

Figure 9. (a) *β*-DPMA in DAC chamber during the pressure measurements; (b) DPMA crystals at atmospheric pressure excited with with 350 nm UV radiation; (c) diagram of reducing the HOMO-LUMO gap with increasing pressure.

Conclusions

Using in-situ single-crystal synchrotron X-ray diffraction, the high-pressure structure of two DPMA polymorphs was determined, *α*-DPMA up to 12.29 GPa and *β*-DPMA up to 10.73 GPa. For the *α*-polymorph, no phase transformation was observed, while for *β*-DPMA, phase transformation occurs at 4 GPa. During the experiments, we observed the fluorescence properties of DPMA crystals, which was changing with the modification of the packing of DPMA molecules, caused by increased pressure. Future plans for this project include fluorescence measurements, quantum calculations, and more detailed structural analysis.

References

(1) Trivedi, B. *Maleic Anhydride*; Springer Science & Business Media, 2013.

(2) Danishefsky, S., T.; Kitahara, T.; Schuda., P. F. Preparation and Diels–Alder Reaction of a Highly Nucleophilic Diene: Trans-1-Methoxy-3-Trimethylsiloxy-1,3-Butadiene and 5β-Methoxycyclohexan-1-One-3β,4β-Dicarboxylic Acid Anhydride. *Org. Synth.* **1983**, *61*, 147–151.

(3) Felthouse, T. R.; Burnett, J. C.; Horrell, B.; Mummey, M. J.; Kuo, Y.-J. Maleic Anhydride, Maleic Acid, and Fumaric Acid. *Kirk-Othmer Encycl. Chem. Technol.* **2001**, No. 10. https://doi.org/10.1002/0471238961.1301120506051220.a01.pub2.

(4) Enomoto, G.; Ogo, Y.; Imoto, T. High Pressure Copolymerization of Styrene with Maleic Anhydride. *Die Makromol. Chemie* **1970**, *138* (1), 19–25. https://doi.org/10.1002/macp.1970.021380103.

(5) Kotsuki, H.; Nishizawa, H.; Kitagawa, S.; Ochi, M.; Yamasaki, N.; Matsuoka, K.; Tokoroyama, T. High Pressure Organic Chemistry. III. Diels-Alder Reaction of Thiophene with Maleic Anhydride. *Bull. Chem. Soc. Jpn.* **1979**, *52* (2), 544–548.

(6) Gaylord, N. G. Poly(Maleic Anhydride). *J. Macromol. Sci. Part C* **1975**, *13* (2), 235–261. https://doi.org/10.1080/15321797508080011.

(7) Neuman, R. C. Pressure Effects as Mechanistic Probes of Orga Radical Reactions. *Acc. Chem. Res.* **1972**, *5* (11), 381–387. https://doi.org/10.1021/ar50059a004.

(8) Jenner, G. High Pressure Kinetic Investigations in Organic and Macromolecular Chemistry. *Angew. Chemie Int. Ed. English* **1975**, *14* (3), 137–143.

(9) Jayaraman, A. Diamond Anvil Cell and High-Pressure Physical Investigations. *Rev. Mod. Phys.* **1983**, *55* (1), 65–108. https://doi.org/10.1103/RevModPhys.55.65.

(10) Katrusiak, A. Lab in a DAC - High-Pressure Crystal Chemistry in a Diamond-Anvil Cell. *Acta Crystallogr. Sect. B Struct. Sci. Cryst. Eng. Mater.* **2019**, *75*, 918–926. https://doi.org/10.1107/S2052520619013246.

(11) Jenssen, E. Krystallform Einiger Organischer Substanzen. *Z. Kryst. logr. Miner.* **1893**, *21*, 180–181.

(12) Über, X.; Anhydrids, D. XXXVIII. Über Dimorphie Und Krystallform Des Diphenylmaleünsäiire - Anhydrids. *Zeitschrift für Krist. Mater.* **1912**, *50* (1–6), 576–581.

(13) Bragg, W. L. The Structure of Some Crystals as Indicated by Their Diffraction of X-Rays. *Proc. R. Soc. London. Ser. A* **1913**, *89* (610), 248–277.

(14) Meents, A.; Kutzke, H.; Jones, M. J.; Wickleder, C.; Klapper, H. Polymorphs of 2 , 3-Diphenyl Maleic Acid Anhydride and 2 , 3-Diphenyl Maleic Imide : Synthesis , Crystal Structures , Lattice Energies and Fluorescence. *Zeitschrift für Krist. - Cryst. Mater.* **2005**, *220* (7), 626–638.

(15) Yoon, M.; Kim, Y. H.; Cho, D. W.; Suh, I. H.; Lee, J. H.; Ryu, B. Y.; Park, J. R. 2,3-Diphenylmaleic Anhydride, an Analogue of Cis-Stilbene. *Acta Crystallogr. Sect. C Cryst. Struct. Commun.* **1995**, *51* (7), 1374–1377. https://doi.org/10.1107/s0108270194013892.

(16) Mei, X.; Wang, J.; Zhou, Z.; Wu, S.; Huang, L.; Lin, Z.; Ling, Q. Diarylmaleic Anhydrides: Unusual Organic Luminescence, Multi-Stimuli Response and Photochromism. *J. Mater. Chem. C* **2017**, *5* (8), 2135–2141. https://doi.org/10.1039/c6tc05519b.

(17) Letoullec, R.; Pinceaux, J. P.; Loubeyre, P. The Membrane Diamond Anvil Cell: A New Device For Generating Continuous Pressure And Temperature Variations. *High Press. Res.* **1988**, *1* (1), 77–90. https://doi.org/10.1080/08957958808202482.

(18) Piermarini, G. J.; Block, S.; Barnett, J. D.; Forman, R. A. Calibration of the Pressure Dependence of the R1ruby Fluorescence Line to 195 Kbar. *J. Appl. Phys.* **1975**, *46* (6), 2774–2780. https://doi.org/10.1063/1.321957.

(19) Mao, H. K.; Xu, J. A.; Bell, P. M. Calibration of Ruby Pressure Gauge to 800 Kbar under Quasi-hydrostatic Conditions. *J. Geophys. Res.* **1986**, *91* (B5), 4673–4676.

(20) Rigaku Oxford Diffraction. CrysAlisPro Software System.

(21) Sheldrick, G. M. A Short History of SHELX. *Acta Crystallogr. Sect. A Found. Crystallogr.* **2008**, *64* (1), 112–122. https://doi.org/10.1107/S0108767307043930.

(22) Sheldrick, G. M. Crystal Structure Refinement with SHELXL . *Acta Crystallogr. Sect. C Struct. Chem.* **2015**, *71* (1), 3–8. https://doi.org/10.1107/s2053229614024218.

(23) Dolomanov, O. V.; Bourhis, L. J.; Gildea, R. J.; Howard, J. A. K.; Puschmann, H. OLEX2: A Complete Structure Solution, Refinement and Analysis Program. *J. Appl. Crystallogr.* **2009**, *42* (2), 339–341. https://doi.org/10.1107/S0021889808042726.

(24) Macrae, C. F.; Edgington, P. R.; McCabe, P.; Pidcock, E.; Shields, G. P.; Taylor, R.; Towler, M.; Van De Streek, J. Mercury: Visualization and Analysis of Crystal Structures. *J. Appl. Crystallogr.* **2006**, *39* (3), 453–457. https://doi.org/10.1107/S002188980600731X.

(25) Wang, X.; Wu, Y.; Liu, Q.; Li, Z.; Yan, H.; Ji, C.; Duan, J.; Liu, Z. Aggregation-Induced Emission (AIE) of Pyridyl-Enamido-Based Organoboron Luminophores. *Chem. Commun.* **2015**, *51* (4), 784–787. https://doi.org/10.1039/C4CC07451C.